



*J. Serb. Chem. Soc.* 75 (11) 1559–1574 (2010)  
JSCS–4076

## Comparative study of ethanol oxidation at Pt-based nanoalloys and UPD-modified Pt nanoparticles

AMALIJA V. TRIPKOVIĆ<sup>\*#</sup>, JELENA D. LOVIĆ<sup>#</sup> and KSENIJA DJ. POPOVIĆ<sup>#</sup>

*ICTM – Institute of Electrochemistry, University of Belgrade, Njegoševa 12,  
P.O. Box 473, 11000 Belgrade, Serbia*

(Received 19 May, revised 30 June 2010)

**Abstract:** The activity of two alloys, Pt<sub>3</sub>Sn/C and Pt<sub>3</sub>Ru<sub>2</sub>/C, was compared with the activity of Pt/C modified with corresponding amounts of Sn<sub>UPD</sub> (≈25 %) and Ru<sub>UPD</sub> (≈40 %) in the oxidation of ethanol. Pt<sub>3</sub>Sn/C, Pt<sub>3</sub>Ru<sub>2</sub>/C and Pt/C catalysts were characterized by XRD analysis. To establish the activity and stability of the catalysts, potentiodynamic, quasi steady-state and chronoamperometric measurements were performed. Both alloys are more active than Sn<sub>UPD</sub>- or Ru<sub>UPD</sub>-modified Pt/C catalysts. The electronic effect determining dominantly the activity of Pt<sub>3</sub>Sn/C is the main reason for its higher activity compared to Pt<sub>3</sub>Ru<sub>2</sub>/C. Since Sn<sub>UPD</sub> and Ru<sub>UPD</sub> do not provoke any significant modification of electronic environment, both modified Pt/C catalysts were less active than the corresponding alloys. More pronounced difference in activity between Pt<sub>3</sub>Sn/C and Sn<sub>UPD</sub>-modified Pt/C than between Pt<sub>3</sub>Ru<sub>2</sub>/C and Ru<sub>UPD</sub>-modified Pt/C is caused by the electronic effect in Pt<sub>3</sub>Sn/C. The high activity of Pt<sub>3</sub>Sn/C modified with a small amount of Sn<sub>UPD</sub> (≈10 %) can be explained by combining the electronic effect, causing less strongly bonded adsorbate on Pt sites and easier mobility of the Sn<sub>UPD</sub>, with an enhanced amount of oxygen-containing species on the Sn sites, resulting finally in a reinforcement of the bi-functional mechanism.

**Keywords:** ethanol oxidation; platinum–tin nanocatalyst; platinum–ruthenium nanocatalyst, platinum nanocatalyst; underpotential deposition.

### INTRODUCTION

Ethanol is promising fuel for direct alcohol low temperature fuel cells due to its low toxicity, high energy density, mass production from renewable sources and easy storage and transportation. However, the lack of an efficient and selective anode catalyst able to break the C–C bond providing complete oxidation to CO<sub>2</sub> with an exchange of 12 e<sup>-</sup> per molecule and to oxidize the adsorbed fragments

\* Corresponding author. E-mail: amalija@tmf.bg.ac.rs

# Serbian Chemical Society member.

doi: 10.2298/JSC100519093T

produced by ethanol dissociation is, at present, the main problem for a practical use of ethanol in a direct ethanol fuel cell (DEFC).

Despite of fact that platinum is generally known as one of the best electrocatalysts for alcohol oxidation at low temperatures, it has limited capability for C–C bond scission and is easily poisoned by CO and other carboneous intermediates.<sup>1–5</sup> To improve its electrocatalytic activity, especially at potentials of technical interest ( $E < 0.6$  V vs. RHE), Pt is modified by the addition of transition metals, providing oxygen-containing species at low potentials which facilitate the oxidative removal of poisoning species through a bifunctional mechanism.<sup>6</sup> The addition of the second metal to platinum (by underpotential deposition or alloying) creates bimetallic catalysts and changes the electronic and structural properties of the base material thereby influencing its catalytic properties. It also alters the number of large Pt ensembles on platinum surfaces, which are important for site demanding processes such as C–C bond cleavage. All these effects influence ethanol oxidation on bimetallic catalysts.

Of all other studied bimetallic catalysts, PtSn/C and PtRu/C catalysts demonstrated the best performance in ethanol oxidation.<sup>7–15</sup>

The electronic effect induced by charge transfer from Sn to Pt was reflected as a negative shift in the Pt 4f binding energies in the XPS spectra of various PtSn/C catalysts.<sup>16</sup> This finding was supported by 1.1 eV shift in the X-ray near edge spectrum (XANES)<sup>17</sup> as well as by X-ray absorption spectroscopic studies (XAS), which demonstrated a partial filling of the Pt 5d-bands.<sup>18</sup>

The relevant results obtained for PtRu/C catalysts by means of different spectroscopic techniques are rather controversial. The XAS spectra revealed electron transfer from Pt to Ru in Pt–Ru/C catalysts,<sup>18</sup> while, on the contrary, the XPS data showed no significant electronic effect in Pt–Ru alloys.<sup>16</sup> The latter results were explained by the similar electronegativity values for Pt and Ru, in contrast to the values for Pt and Sn which differ appreciably.

Incorporation of Sn atoms in the *fcc* Pt lattice enhances the Pt–Pt bond distance, thereby altering the structural characteristic of the base metal. The extended Pt–Pt distance could facilitate the dissociative adsorption of ethanol molecules and promote the reaction.<sup>15,19–21</sup> However, the reduced Pt–Pt distance caused by the addition of Ru to Pt should not be favorable for dissociative adsorption of ethanol.<sup>10,15,19</sup>

From the viewpoint of the role of an ensemble effect in the oxidation of ethanol on PtRu/C<sup>7</sup> and PtSn/C<sup>22</sup> catalysts with different ratios between Pt and the alloying atoms, it was suggested that an increase of the Ru or Sn content may cause a negative effect on the selectivity of the catalysts towards CO<sub>2</sub> formation by decreasing the Pt ensembles required for the dissociative adsorption of ethanol.

Recently, the activity of Pt–Sn/C and Pt–Ru/C in ethanol oxidation was correlated with the degree of alloying. Although the results reported so far are ge-

nerally not unambiguous, most of them indicate that highly alloyed catalysts promote ethanol oxidation.<sup>8,23–27</sup>

Underpotential deposition (UPD) of Sn or Ru at Pt/C does not significantly perturb Pt structurally or electronically, as was shown in spectroscopic studies.<sup>16,18,28</sup> The catalytic action of both atoms was associated mostly with their ability to adsorb oxygenated species at lower potentials than Pt, permitting the bifunctional mechanism to proceed.

In this work, ethanol oxidation was studied at two alloys, Pt<sub>3</sub>Sn/C and Pt<sub>3</sub>Ru<sub>2</sub>/C, as well as at a Pt/C catalyst modified with the corresponding amounts of Sn<sub>UPD</sub> (25 %) and Ru<sub>UPD</sub> (40 %). This comparative investigation based on the effects influencing the catalytic properties of these electrodes enabled a better understanding of the differences in the activities of the alloys, as well as those of the alloys and Pt/C modified by underpotentially deposited Sn and Ru. This approach, which to the best of our knowledge, has not been used so far, resulted finally in the comprehension of the superior activity of the catalyst created by modification of Pt<sub>3</sub>Sn/C with a small amount of Sn<sub>UPD</sub> ( $\approx 10\%$ ).

## EXPERIMENTAL

### *Electrode preparation*

Commercially available Pt-based catalysts supported on high surface area carbon were used: Pt<sub>3</sub>Sn/C (20 wt. %) provided by E-Tek, and Pt<sub>3</sub>Ru<sub>2</sub>/C (33.5 wt. %) and Pt/C (47.5 wt. %) provided by Tanaka Precious Metals Group (Kikinzoku International K.K). The catalysts were applied to a glassy carbon substrate in the form of a thin-film.<sup>10</sup> A suspension of 5 mg of the catalyst in a mixture of 1 ml water, 1 ml ethanol and 50  $\mu$ l of a 5 % aqueous Nafion solution was prepared in an ultrasonic bath and 10  $\mu$ l of the suspension was placed onto the substrate (5 mm diameter) and dried at room temperature to form a homogenous catalyst layer. The resulting metal loading was 25  $\mu$ g cm<sup>-2</sup>.

To avoid the contribution of any other anions, Sn or Ru adlayers were prepared by holding freshly prepared electrodes at  $-0.2$  V in 0.1 M HClO<sub>4</sub> solution containing Sn or Ru ions, generated by dissolution of Sn or Ru from the alloy matrix during cycling (20 cycles) of the Pt<sub>3</sub>Sn/C and Pt<sub>3</sub>Ru<sub>2</sub>/C electrodes up to 0.70 V or 1.10 V, respectively. The Sn or Ru modified electrode was then rinsed with water and transferred to the electrochemical cell.

### *Characterization of the catalysts*

The Pt/C, Pt<sub>3</sub>Ru<sub>2</sub>/C and Pt<sub>3</sub>Sn/C catalysts were characterized by X-ray diffraction (XRD) analysis. The XRD measurements were realized using a Siemens D5005 (Bruker-AXS) diffractometer with a Cu K $\alpha$  source operating at 40 mA and 40 kV and a graphite monochromator.

The quantitative analysis of the phase content and crystallite size calculations were performed by multiphase Rietveld refinement using Topas software and the Fundamental Parameters approach for the modeling of the peak shape. The Pt(220) diffraction peak was used to calculate the average crystallite size according to the Scherrer Equation.

### *Electrochemical measurements*

Electrochemical measurements were performed at room temperature in a nitrogen-purged 0.1 M HClO<sub>4</sub> solution in a standard three compartment electrochemical cell with a Pt wire

as the counter electrode and a saturated calomel electrode (SCE) as the reference. The employed reagents were of p.a. purity (Merck) and the solutions were prepared with high purity water ("Millipore", 18 M $\Omega$  cm resistivity). Ethanol (0.5 M) was added to the solution while holding the electrode potential at  $-0.2$  V. The catalytic activity was measured using the potentiodynamic (sweep rate 20 mV s $^{-1}$ ), quasi-steady-state (sweep rate 1 mV s $^{-1}$ ) and chronoamperometric methods. The current–time transient curves were recorded during 30 min upon the immersion of the electrode in the solution at  $-0.2$  V and holding for 2 s prior to stepping at 0.2 V. For the CO stripping measurements, pure CO was bubbled through the electrolyte for 20 min while keeping the electrode potential at  $-0.2$  V vs. SCE. After purging the electrolyte with N $_2$  for 30 min to eliminate the dissolved CO, the adsorbed CO was oxidized in an anodic scan (20 mV s $^{-1}$ ). Two subsequent voltammograms were also recorded to verify the completeness of the CO oxidation.

A VoltaLab PGZ402 (Radiometer Analytical, Lyon, France) was used in the electrochemical experiments.

The potentials are given *versus* SCE. The current densities are normalized to the active surface area.

The active surface area for Pt $_3$ Sn/C, Pt $_3$ Ru $_2$ /C and Pt/C was calculated from the the charge of CO stripping, assuming 420  $\mu$ C cm $^{-2}$  for a CO monolayer (Fig. 1). The CO stripping voltammograms were corrected for the background currents to eliminate the contribution of the double layer charge, as well as Sn and Ru oxidation charges.<sup>29</sup>

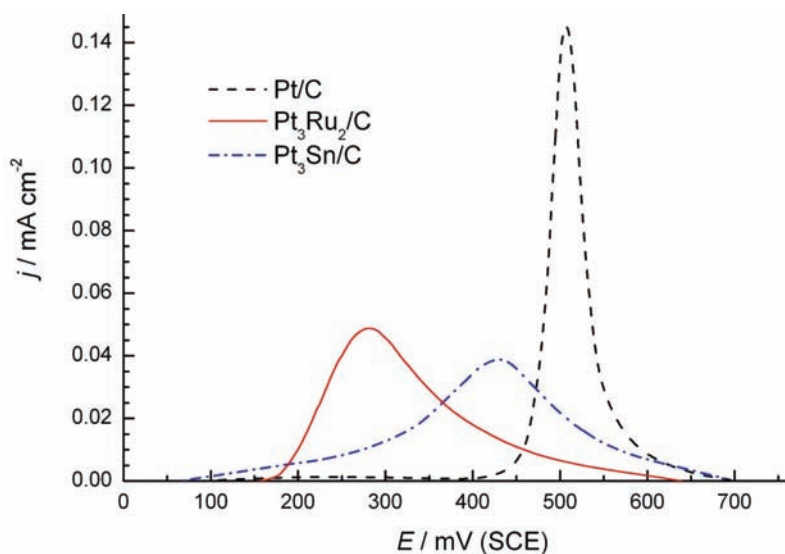


Fig. 1. CO stripping voltammograms at Pt/C, Pt $_3$ Ru $_2$ /C and Pt $_3$ Sn/C catalysts in 0.1 M HClO $_4$  corrected for the background current;  $\nu = 20$  mV s $^{-1}$ .

## RESULTS AND DISCUSSION

### Catalysts characterization

The X-ray diffraction patterns of Pt $_3$ Sn/C, Pt $_3$ Ru $_2$ /C and Pt/C catalysts are presented in Fig. 2. All samples display four characteristic peaks of the face cen-

tered cubic (*fcc*) crystalline structure of Pt, *i.e.*, (111), (200), (220) and (311). No peaks for either Sn or Pt oxides were found. However, this does not mean that they were not present; they could be present but in undetectably small amounts or in an amorphous form. The poorly resolved peak at  $\approx 43.8^\circ$  on the diffractogram for the Pt<sub>3</sub>Ru<sub>2</sub>/C catalyst is assigned to the hexagonal Ru phase (*hcp*). Two broad peaks that appeared at 14.0 and 30.9° are related to the carbon support material.

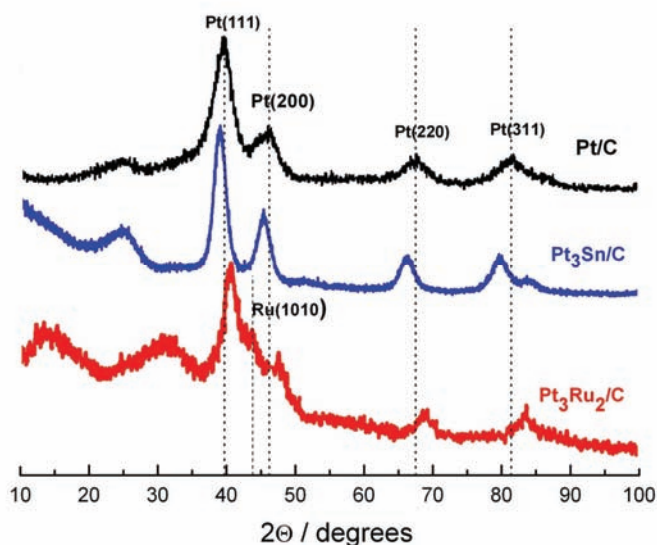


Fig. 2. XRD Patterns of Pt<sub>3</sub>Sn/C, Pt<sub>3</sub>Ru<sub>2</sub>/C and Pt/C catalysts. Vertical lines represent the position of the peaks of pure Pt and pure Ru.

Addition of Sn or Ru to Pt leads to an expansion or contraction of the Pt lattice, respectively, caused by their different atomic sizes in respect to that of Pt ( $R_{\text{Sn}} = 1.61 \text{ \AA}$ ,  $R_{\text{Ru}} = 1.34 \text{ \AA}$ ,  $R_{\text{Pt}} = 1.39 \text{ \AA}$ ), which correspondingly shifts the peaks in opposite directions compared to Pt/C.

The lattice parameters calculated from the (220) peak as well as the mean crystallite diameters are listed in Table I. The atomic fractions of Sn and Ru ( $x_{\text{Me}}$ ) and alloying degree ( $M_{\text{alloy}} / \%$ ) calculated *via* the Vegard law<sup>8</sup> are also given in Table I. The atomic fraction of Sn,  $x_{\text{Sn}} = 0.243$  is close to the nominal content of 0.25 in the Pt<sub>3</sub>Sn/C catalyst, indicating that almost all the Sn atoms

TABLE I. XRD Analysis of Pt/C, Pt<sub>3</sub>Ru<sub>2</sub>/C and Pt<sub>3</sub>Sn/C catalysts

Catalysts	Nominal content (Pt:Me)	Mean crystallite diameter, nm	Lattice parameter nm	$x_{\text{Me}}$	$M_{\text{alloy}} \%$
47.5 wt. % Pt/C	–	3.9	0.39166	–	–
33.5 wt. % Pt <sub>3</sub> Ru <sub>2</sub> /C	60:40	4.5	0.3871	0.368	87.4
20 wt. % Pt <sub>3</sub> Sn/C	75:25	5.2	0.398385	0.243	96.4

were alloyed to Pt. The atomic fraction of Ru,  $x_{\text{Ru}} = 0.368$ , is slightly below the nominal content of 0.4 in  $\text{Pt}_3\text{Ru}_2/\text{C}$ , implying that most of the Ru atoms were incorporated in the *fcc* Pt structure. This was confirmed by the corresponding alloying degrees of 96.4 % for  $\text{Pt}_3\text{Sn}/\text{C}$  and 87.4 % for  $\text{Pt}_3\text{Ru}_2/\text{C}$ .

#### Ethanol oxidation

The polarization curves for ethanol oxidation on  $\text{Pt}_3\text{Sn}/\text{C}$ ,  $\text{Pt}_3\text{Ru}_2/\text{C}$  and  $\text{Pt}/\text{C}$  catalysts in acid solution are given in Fig. 3. The positive potentials were limited to 0.3 V to avoid any Sn or Ru dissolution.

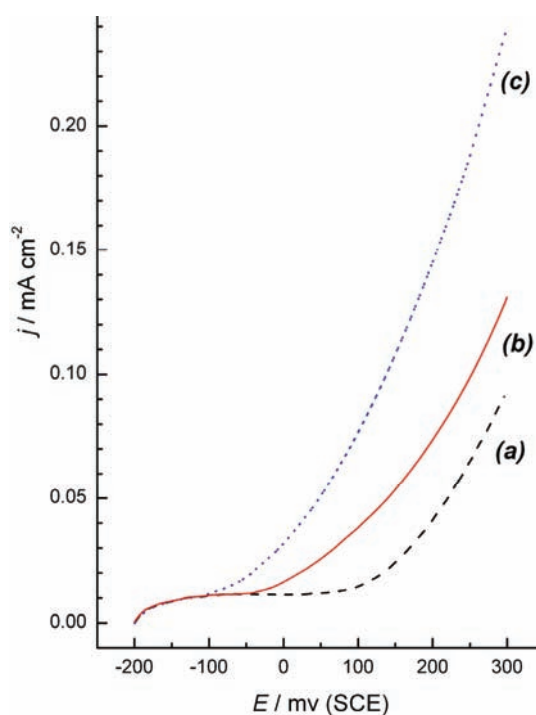


Fig. 3. Potentiodynamic curves for the oxidation of 0.5 M  $\text{C}_2\text{H}_5\text{OH}$  at  $\text{Pt}/\text{C}$  (curve a),  $\text{Pt}_3\text{Ru}_2/\text{C}$  (curve b) and  $\text{Pt}_3\text{Sn}/\text{C}$  (curve c) catalysts in 0.1 M  $\text{HClO}_4$ ;  $\nu = 20 \text{ mV s}^{-1}$ .

The  $\text{Pt}/\text{C}$  catalyst exhibited a low activity (curve a). The reaction commenced at  $\approx 0.1 \text{ V}$  when the dissociative adsorption of water occurred, providing  $\text{OH}_{\text{ad}}$  species<sup>30</sup> needed for the oxidation of adsorbate containing  $\text{C}_1$  fragments (mostly  $\text{CO}_{\text{ad}}$ <sup>11,14</sup> and  $\text{CH}_x$ <sup>5</sup>) and  $\text{C}_2$  fragments generated by the dissociative adsorption of ethanol.<sup>3,8</sup>

Both alloys were more active than  $\text{Pt}/\text{C}$ . The onset potentials on the  $\text{Pt}_3\text{Ru}_2/\text{C}$  (curve b) and  $\text{Pt}_3\text{Sn}/\text{C}$  (curve c) catalysts are shifted to less positive potentials with respect to  $\text{Pt}/\text{C}$  by  $\approx 0.15$  and  $\approx 0.25 \text{ V}$ , respectively. The catalytic action of Sn or Ru in the corresponding Pt-based alloys was correlated generally by their ability to dissociate water at lower potentials than Pt, enabling the bifunctional



mechanism between the adsorbate on the Pt and the OH species adsorbed on the added metals to proceed.<sup>6</sup> However, the superior activity of Pt<sub>3</sub>Sn/C with respect to Pt<sub>3</sub>Ru<sub>2</sub>/C catalyst requires further analysis.

Alloying Sn to Pt causes an electronic modification due to the Pt–Sn interaction. An electronic modification in the unfilled d-band states of Pt atoms in various PtSn catalysts has been evidenced by spectroscopic techniques.<sup>16–18,22</sup> Characteristic for Sn is the decrease of the local density of states at the Fermi level, which is in direct correspondence with the lowering of the energy of the d-band center. Therefore, CO binds more weakly on a Pt<sub>3</sub>Sn surface than on a pure Pt surface, which is in accordance with the downshift of the d-band centers of the platinum atoms.<sup>31,32</sup> The Sn atom is not a strong acceptor of electrons from water molecules and forms a weak bond with OH.<sup>22,33</sup> Both phenomena should be beneficial for ethanol oxidation.

Incorporation of Sn atoms in the *fcc* Pt lattice leads to an expansion of the lattice parameter, as revealed by XRD analysis (Table I), changing the structure of the Pt-based material. The elongation of lattice parameter may facilitate C–C bond cleavage thus improving the catalytic activity.<sup>15,20,21</sup> A DFT calculation supports this assumption, indicating that surface transition species originating from ethanol are sensitive to the bond length and angle.<sup>34</sup>

As the Pt<sub>3</sub>Sn/C catalyst had the high alloying degree of 96.4 %, it is reasonable to assume that both effects, electronic and structural, could be the origin of its high activity. On the other hand, C–C bond cleavage is a site demanding process requiring at least two adjacent (ensemble) binding Pt sites as the C–C bond length is 1.5 Å and the atomic diameter of Pt is 1.39 Å. This means that larger Pt ensembles are required for C–C bond breakage, while on smaller Pt ensembles, incomplete ethanol oxidation to acetaldehyde and acetic acid should be promoted. The number of the large Pt ensembles is generally diminished by incorporation of Sn into the Pt lattice, but it may be simultaneously compensated with the structural effect originating from the expansion of the Pt–Pt distance (Table I). However, it should be pointed out that the selectivity of Pt<sub>3</sub>Sn/C or other PtSn/C catalysts towards CO<sub>2</sub> formation was not improved significantly with respect to a Pt/C catalyst.<sup>4,7,8,10,23</sup>

Electron transfer from Pt to Ru in the Pt<sub>3</sub>Ru<sub>2</sub>/C catalyst<sup>18</sup> decreases the bond strength between Pt and adsorbate produced from ethanol.<sup>32</sup> Moreover, the decreased Pt–Pt bond distance seems to be unfavorable for C–C bond cleavage.<sup>10</sup>

If electronic and structural effects are not beneficial for ethanol oxidation, than the promotion of catalytic activity of Pt<sub>3</sub>Ru<sub>2</sub>/C with respect to Pt/C arises mainly from the ability of Ru atoms to dissociate water at lower potentials compared to Pt, providing oxygen-containing species to oxidize the adsorbed fragments generated from ethanol. However, although the capability of Ru atoms to dissociate water is larger than Sn atoms,<sup>16</sup> Pt<sub>3</sub>Ru<sub>2</sub>/C is significantly less active

than Pt<sub>3</sub>Sn/C in ethanol oxidation most likely due to the slightly stronger bonded adsorbate, *i.e.*, higher poisoning of the surface.

Electronic effect dominantly determined the activity of the Pt<sub>3</sub>Sn/C catalyst in ethanol oxidation and it is the main reason for its higher activity with respect to Pt<sub>3</sub>Ru<sub>2</sub>/C.<sup>35</sup> The structural or ensemble effects seems to be less important, since the selectivity for oxidation to CO<sub>2</sub> is not significantly increased on both catalysts compared to Pt/C.<sup>19</sup>

The stability of the catalysts was studied in chronoamperometric experiments (Fig. 4). The highest initial current density at 0.2 V on Pt<sub>3</sub>Sn/C related to the other two catalysts is in accordance with the potentiodynamic measurements (Fig. 3). The currents decay rapidly at Pt/C and Pt<sub>3</sub>Ru<sub>2</sub>/C catalysts, reaching their steady state values within a few minutes. On the other hand, the initial current decreases slightly at Pt<sub>3</sub>Sn/C and stabilizes in the experimental period of time at a value which is about two times higher than at the Pt<sub>3</sub>Ru<sub>2</sub>/C catalyst. The Pt<sub>3</sub>Sn/C catalyst is evidently less poisoned than Pt<sub>3</sub>Ru<sub>2</sub>/C or Pt/C.

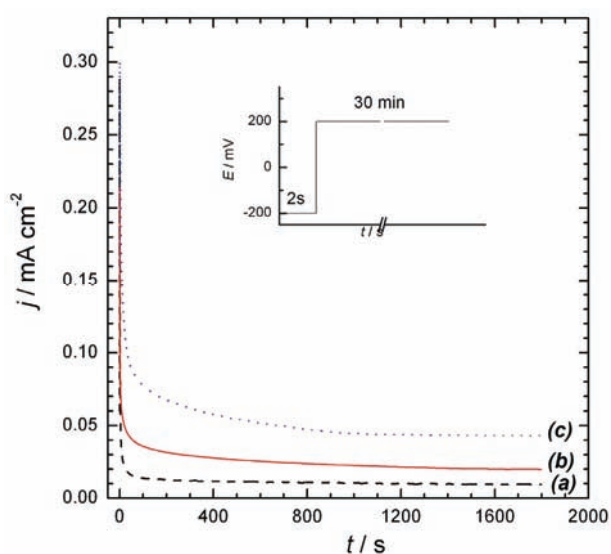


Fig. 4. Chronoamperometric curves for the oxidation of 0.5 M C<sub>2</sub>H<sub>5</sub>OH at 0.2 V at Pt/C (curve a), Pt<sub>3</sub>Ru<sub>2</sub>/C (curve b) and Pt<sub>3</sub>Sn/C (curve c) catalysts in 0.1 M HClO<sub>4</sub>.

Ethanol oxidation at Pt<sub>3</sub>Sn/C, Pt/C and the Sn<sub>UPD</sub>-modified Pt/C and Pt<sub>3</sub>Sn/C catalysts and the corresponding basic voltammograms are displayed in Fig. 5.

The decrease of charge in the hydrogen region of  $\approx 25\%$  between Pt/C and the Sn<sub>UPD</sub>-modified Pt/C catalyst (Fig. 5A) can be related to the coverage with Sn<sub>UPD</sub>, assuming that hydrogen does not adsorb on Sn.<sup>36</sup>

The activity of Pt/C catalyst was improved by the Sn<sub>UPD</sub> layer (Fig. 5C). The reaction commences at  $\approx 0.0$  V (curve a'), *i.e.*, at  $\approx 0.1$  V less positive potentials relative to Pt/C (curve a).



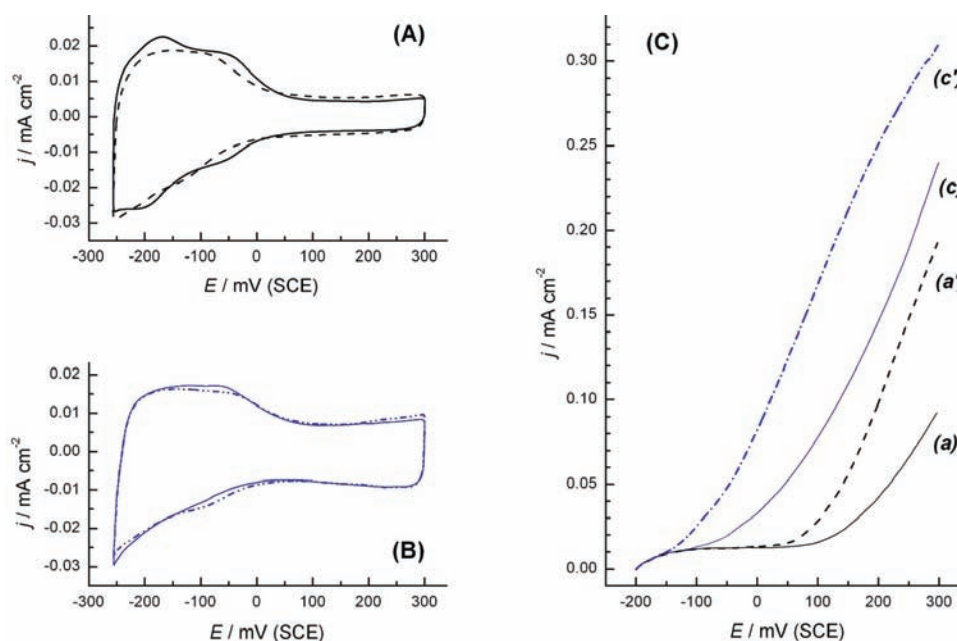


Fig. 5. (A) Basic voltammograms of Pt/C (solid line) and Pt/C modified with 25 %  $\text{Sn}_{\text{UPD}}$  (dash line); (B) basic voltammograms of the  $\text{Pt}_3\text{Sn}/\text{C}$  electrode (solid line) and  $\text{Pt}_3\text{Sn}/\text{C}$  modified with 10 %  $\text{Sn}_{\text{UPD}}$  (dash-dot line); (C) potentiodynamic curves for the oxidation of 0.5 M  $\text{C}_2\text{H}_5\text{OH}$  in 0.1 M  $\text{HClO}_4$  at Pt/C (curve a), at Pt/C modified with 25 %  $\text{Sn}_{\text{UPD}}$  (curve a'), at  $\text{Pt}_3\text{Sn}/\text{C}$  (curve c) and at  $\text{Pt}_3\text{Sn}/\text{C}$  modified with 10 %  $\text{Sn}_{\text{UPD}}$  (curve c');  $\nu = 20 \text{ mV s}^{-1}$ .

Comparison of  $\text{Pt}_3\text{Sn}/\text{C}$  containing  $\approx 25$  at. % of Sn (curve c) with Pt/C modified by the same amount of  $\text{Sn}_{\text{UPD}}$  (curve a') reveals clearly that the alloy is considerably more active. The onset of the reaction at  $\text{Pt}_3\text{Sn}/\text{C}$  is shifted by more than 0.1 V to less positive potentials and the current densities are enhanced. Spectroscopic analysis of  $\text{Sn}_{\text{UPD}}$  on Pt/C shows that the  $\text{Sn}_{\text{UPD}}$  interacts with oxygen species similarly as in  $\text{Pt}_3\text{Sn}/\text{C}$  alloy, but the underpotential deposition of Sn on Pt/C induces much smaller electronic changes in Pt/C than in  $\text{Pt}_3\text{Sn}/\text{C}$ .<sup>28</sup> This means that  $\text{Sn}_{\text{UPD}}$  does not interfere remarkably with the ability of Pt to adsorb strongly ethanol or the adsorbate generated by ethanol dissociation, which should be the main reason for the lower activity of the  $\text{Sn}_{\text{UPD}}$  modified Pt/C with respect to  $\text{Pt}_3\text{Sn}/\text{C}$ .

The small amount of Sn ( $\approx 10$  %) electrodeposited on  $\text{Pt}_3\text{Sn}/\text{C}$  (Fig. 5B) promotes the activity of the alloy (Fig. 5C, curve c'), creating a powerful catalyst for ethanol oxidation as was shown in the literature.<sup>37</sup> The high activity of this catalyst can be explained by combining the electronic effect, causing less strongly bonded adsorbate on the Pt sites, and the easier mobility of  $\text{Sn}_{\text{ad}}$ ,<sup>38</sup> with enhanced amount of oxygen-containing species on the Sn sites, resulting, as a final consequence, in a reinforcement of the bifunctional mechanism.

Using the same approach, ethanol oxidation was examined at  $\text{Pt}_3\text{Ru}_2/\text{C}$  containing 40 % of Ru (Fig. 6B) and compared with the Pt/C catalyst modified with approximately the same amount ( $\approx 40\%$ ) of  $\text{Ru}_{\text{UPD}}$ , (Fig. 6C, curves b and a'', respectively). The decrease of charge in the hydrogen region of  $\approx 40\%$  between  $\text{Ru}_{\text{UPD}}$  modified and unmodified Pt/C catalyst (Fig. 6A) can be attributed to the coverage with  $\text{Ru}_{\text{UPD}}$  on the Pt sites, assuming that the maximal coverage of Ru by H adatoms is  $\approx 15\%$ .<sup>39,40</sup>

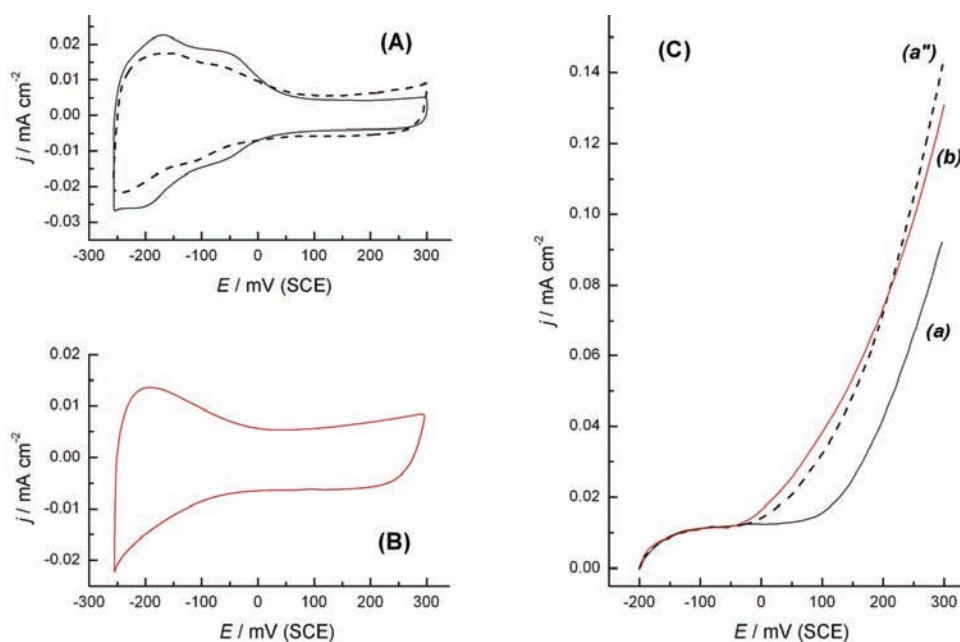


Fig. 6. (A) Basic voltammograms of Pt/C (solid line) and Pt/C modified with 40 %  $\text{Ru}_{\text{UPD}}$  (dash line); (B) basic voltammogram of  $\text{Pt}_3\text{Ru}_2/\text{C}$  electrode; (C) potentiodynamic curves for the oxidation of 0.5 M  $\text{C}_2\text{H}_5\text{OH}$  in 0.1 M  $\text{HClO}_4$  at Pt/C (curve a), at Pt/C modified with 40 %  $\text{Ru}_{\text{UPD}}$  (curve a'') and at  $\text{Pt}_3\text{Ru}_2/\text{C}$  (curve b);  $\nu = 20 \text{ mV s}^{-1}$ .

Inspection of the results given in Fig. 6C shows a significant difference in respect to the corresponding results obtained at  $\text{Pt}_3\text{Sn}/\text{C}$  and  $\text{Sn}_{\text{UPD}}$  modified Pt/C catalysts (Fig. 5C). The substantial easily recognized contrast is the small difference between the activity of  $\text{Pt}_3\text{Ru}_2/\text{C}$  (curve b) and that of the Pt/C modified by the same amount of underpotentially deposited Ru (curve a''). This is reliable proof that electronic or structural effects do not provoke a significant influence on the activity of Ru alloyed Pt catalysts. In this context, the high alloying degree of 87.4 % (Table I) is not as relevant for an estimation of the catalytic properties of  $\text{Pt}_3\text{Ru}_2/\text{C}$  as it is in a case of the  $\text{Pt}_3\text{Sn}/\text{C}$  catalyst. Since underpotential deposition of Ru on Pt/C does not provoke significant electronic changes in Pt/C,<sup>16,18</sup> ethanol oxidation on the respective catalysts obeys the con-

ditions relevant for the bifunctional mechanism. In this sense, the ratio between Pt sites, which adsorb ethanol, and Ru sites, which nucleate oxygen species to oxidize that adsorbate, becomes crucial. The ratio Pt/Ru = 60:40 fulfilled in Pt<sub>3</sub>Ru<sub>2</sub>/C as well as in Pt/C modified by 40 % of Ru<sub>UPD</sub> provide the best catalytic performance.<sup>41</sup> The addition of  $\approx 10\%$  Ru<sub>UPD</sub> on Pt<sub>3</sub>Ru<sub>2</sub>/C or enhancement of the amount of Ru<sub>UPD</sub> on Pt/C at 50 % decreases the activity of both catalysts, respectively (not shown).

The activities of the catalysts studied in ethanol oxidation obtained under quasi-steady state conditions are given in Figs. 7 and 8. In these plots, the cur-

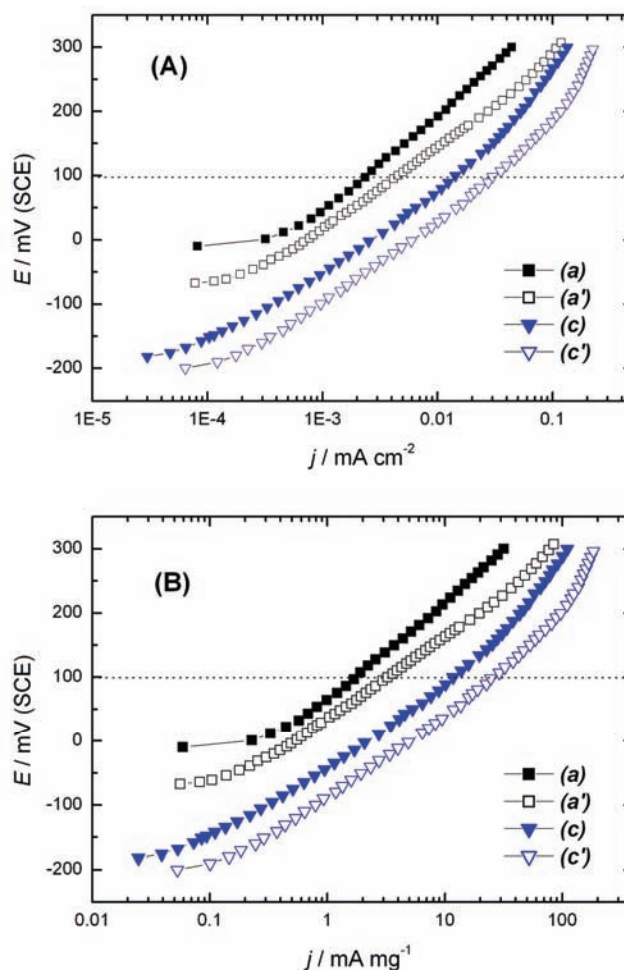


Fig. 7. Tafel plots for the oxidation of 0.5 M C<sub>2</sub>H<sub>5</sub>OH in 0.1 M HClO<sub>4</sub> solution at: Pt/C (curve a), Pt/C modified with 25 % Sn<sub>UPD</sub> (curve a'), Pt<sub>3</sub>Sn/C (curve c) and Pt<sub>3</sub>Sn/C modified with 10 % Sn<sub>UPD</sub> (curve c'). (A) Current density normalized to the active surface area of the respective catalysts; (B) mass specific current density;  $\nu = 1 \text{ mV s}^{-1}$ .

rents are given either as active surface area normalized current densities (Figs. 7A and 8A) or as mass normalized currents (Figs. 7B and 8B). The Pt<sub>3</sub>Sn/C is more active than the Pt/C modified by Sn<sub>UPD</sub> ( $\approx 25\%$ ) catalysts (Fig. 7) and considerably more active than Pt/C. The activity of Pt<sub>3</sub>Ru<sub>2</sub>/C and Pt/C modified by Ru<sub>UPD</sub> ( $\approx 40\%$ ) are similar, but both catalysts are more active than Pt/C (Fig. 8). The activity of the respective catalysts at  $E = 0.1$  V (SCE) summarized in Table II show that the ratio of the activity between the alloys and corresponding Sn<sub>UPD</sub>- or Ru<sub>UPD</sub>-modified Pt/C is generally maintained regardless of whether the currents are given as active surface area or as mass specific currents.

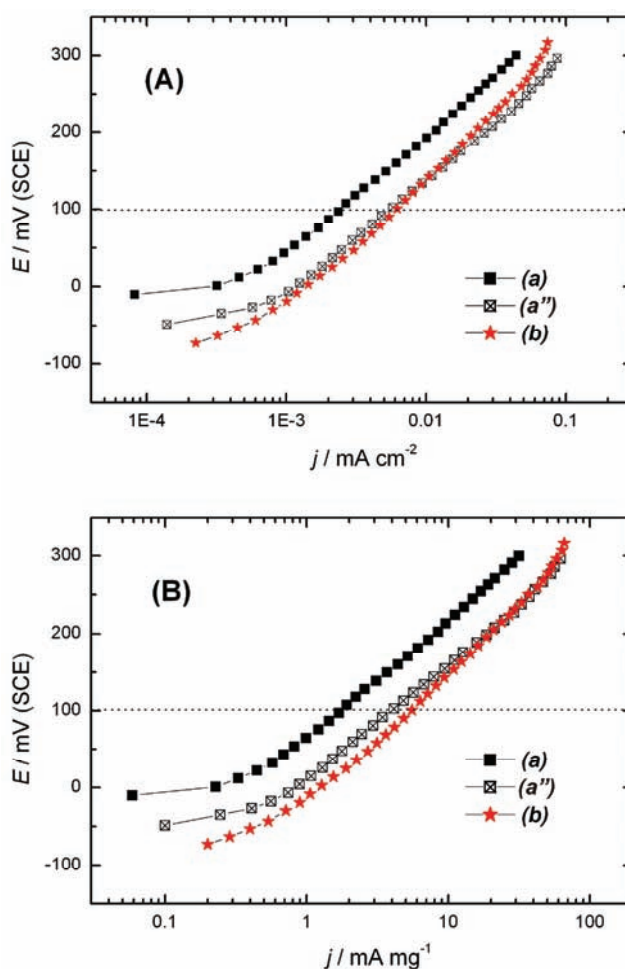


Fig. 8. Tafel plots for the oxidation of 0.5 M C<sub>2</sub>H<sub>5</sub>OH in 0.1 M HClO<sub>4</sub> solution at: Pt/C (curve a), Pt/C modified with 40 % Ru<sub>UPD</sub> (curve a'') and Pt<sub>3</sub>Ru<sub>2</sub>/C (curve b). (A) Current density normalized to the active surface area of the respective catalysts; (B) mass specific current density;  $\nu = 1 \text{ mV s}^{-1}$ .

Pt<sub>3</sub>Sn/C modified by  $\approx 10\%$  Sn<sub>UPD</sub> is the best catalyst studied. Its activity enhanced more than two times in respect to Pt<sub>3</sub>Sn/C catalyst is close to the activity attained at ternary Pt/Rh/SnO<sub>2</sub> catalyst.<sup>42–44</sup>

TABLE II. Activity of the respective catalysts at  $E = 0.1$  V (SCE)

Catalysts	Pt/C	Pt/C + 25 % Sn <sub>UPD</sub>	Pt <sub>3</sub> Sn/C	Pt <sub>3</sub> Sn/C + 10 % Sn <sub>UPD</sub>	Pt <sub>3</sub> Ru <sub>2</sub> /C	Pt/C + 40 % Ru <sub>UPD</sub>
$j / \text{mA mg}^{-1}$	1.69	3.25	11.75	25.6	5.45	4.02
$j / \text{mA cm}^{-2}$	$2.4 \times 10^{-3}$	$4.6 \times 10^{-3}$	$14.2 \times 10^{-3}$	$31.3 \times 10^{-3}$	$6.2 \times 10^{-3}$	$5.5 \times 10^{-3}$

Tafel slopes of  $\approx 120$  mV dec<sup>-1</sup> obtained at Pt<sub>3</sub>Sn/C and Sn<sub>UPD</sub> modified Pt/C catalysts indicate that the first electron transfer could be the rate determining step.<sup>23</sup> Higher Tafel slopes of 140–150 mV dec<sup>-1</sup> at Pt/C, Pt<sub>3</sub>Ru<sub>2</sub>/C and Ru<sub>ad</sub> modified Pt/C catalysts are caused by a large poisoning of Pt.<sup>45</sup>

#### CONCLUSIONS

According to the results obtained in this work dealing with the effects influencing the overall ethanol oxidation on the studied catalysts, the following conclusions can be reached.

Both alloys are more active than Pt/C. Pt<sub>3</sub>Sn/C is more active than Pt<sub>3</sub>Ru<sub>2</sub>/C or the corresponding Sn<sub>UPD</sub>- or Ru<sub>UPD</sub>-modified Pt/C catalysts as revealed from potentiodynamic and quasi steady state measurements. Its high activity originates mainly from the electronic effect causing the weakly bonded adsorbate generated by ethanol adsorption on the Pt sites and the appropriate amount of oxygen-containing species labile bound to Sn to oxidize the adsorbate through the bifunctional mechanism. It was concluded that the promoted OH generation is the primary reason for the enhanced activity towards ethanol oxidation on the Pt<sub>3</sub>Ru<sub>2</sub>/C catalyst.

Since underpotential deposition of Sn or Ru does not provoke any significant electronic effect, both the modified Pt/C catalysts were less active than the corresponding alloys. Accordingly, the more pronounced difference between the Pt<sub>3</sub>Sn/C and the Sn<sub>UPD</sub>-modified Pt/C (25 % Sn) as compared to the difference between Pt<sub>3</sub>Ru<sub>2</sub>/C and the Ru<sub>UPD</sub>-modified Pt/C (40 % Ru) is caused by the electronic effect in Pt<sub>3</sub>Sn/C.

Modification of Pt<sub>3</sub>Sn/C with a small amount of Sn<sub>UPD</sub> ( $\approx 10\%$ ) creates a powerful catalyst for overall ethanol oxidation.

*Acknowledgements.* This work was financially supported by the Ministry of Science and Technological Development of the Republic of Serbia, Contract No. H-142056.

## ИЗВОД

УПОРЕДНО ИСПИТИВАЊЕ ОКСИДАЦИЈЕ ЕТАНОЛА НА ПЛАТИНСКИМ  
НАНОЛЕГУРАМА И Pt НАНОЧЕСТИЦАМА МОДИФИКОВАНИМ  
ПОДПОТЕНЦИЈАЛНОМ ДЕПОЗИЦИЈОМ

АМАЛИЈА В. ТРИПКОВИЋ, ЈЕЛЕНА Д. ЛОВИЋ и КСЕНИЈА Ђ. ПОПОВИЋ

*ИХТМ – Центар за електрохемију, Универзитет у Београду, Њевошева 12, б. бр. 473, 11000 Београд*

Активност две легуре, Pt<sub>3</sub>Sn/C и Pt<sub>3</sub>Ru<sub>2</sub>/C, упоређене су са активностима Pt/C модификованим одговарајућим количинама Sn<sub>UPD</sub> (≈ 25 %) или Ru<sub>UPD</sub> (≈ 40 %) у реакцији оксидације етанола. Катализатори су окарактерисани дифракцијом X-зрака (XRD) и одређен је степен легирања. Њихова активност и стабилност испитивана је потенциодинамичким, квази-стационарним и хроноамперометријским мерењима. Добијени резултати су показали да су обе легуре активније од Sn<sub>UPD</sub> и Ru<sub>UPD</sub> модификованог Pt/C катализатора. Активност Pt<sub>3</sub>Sn/C катализатора одређена је значајним електронским ефектом, што је и главни разлог његове веће активности у односу на Pt<sub>3</sub>Ru<sub>2</sub>/C. Одсуство електронског ефекта код Sn<sub>UPD</sub> и Ru<sub>UPD</sub> модификованог Pt/C катализатора чини ове електроде мање активним од одговарајућих легура, тј. од Pt<sub>3</sub>Sn/C и Pt<sub>3</sub>Ru<sub>2</sub>/C. Већа разлика у активности између Pt<sub>3</sub>Sn/C и Sn<sub>UPD</sub> модификованог Pt/C катализатора него између Pt<sub>3</sub>Ru<sub>2</sub>/C и Ru<sub>UPD</sub> модификованог Pt/C катализатора изазвана је електронским ефектом у Pt<sub>3</sub>Sn/C катализатору. Велика активност Pt<sub>3</sub>Sn/C катализатора модификованог малом количином Sn<sub>UPD</sub> (≈ 10 %) може се објаснити комбинацијом електронског ефекта, тј. слабијом везом адсорбата на Pt местима и већом мобилношћу Sn<sub>UPD</sub>, и повећаном количином OH<sub>ад</sub> честица на Sn местима, што као крајњи резултат има побољшање бифункционалног механизма реакције.

(Примљено 19. маја, ревидирано 30. јуна 2010)

## REFERENCES

1. G. A. Camara, T. Iwasita, *J. Electroanal. Chem.* **578** (2005) 315
2. H. Wang, Z. Jusys, R. J. Behm, *J. Phys. Chem. B* **108** (2004) 19413
3. M. H. Shao, R. R. Adžić, *Electrochim. Acta* **50** (2005) 2415
4. C. Coutanceau, S. Brimaud, C. Lamy, J.-M. Leger, L. Dubau, S. Rousseau, F. Vigier, *Electrochim. Acta* **53** (2008) 6865
5. S. C. S. Lai, E. F. Kleyn, V. Rosca, M. T. Koper, *J. Phys. Chem. C* **112** (2008) 19080
6. M. Watanabe, S. Motoo, *J. Electroanal. Chem.* **60** (1975) 267
7. H. Wang, Z. Jusys, R. J. Behm, *J. Power Sources* **154** (2006) 351
8. L. Colmenares, H. Wang, Z. Jusys, L. Jiang, S. Yan, G. Q. Sun, R. J. Behm, *Electrochim. Acta* **52** (2006) 221
9. E. Antolini, *J. Power Sources* **170** (2007) 1
10. Q. Wang, G. Q. Sun, L. H. Jiang, Q. Xin, S. G. Sun, Y. X. Jiang, S. P. Chen, Z. Jusys, R. J. Behm, *Phys. Chem. Chem. Phys.* **9** (2007) 2686
11. F. C. Simoes, D. M. dosAnjos, F. Vigier, J.-M. Leger, F. Hahn, C. Coutanceau, E. R. Gonzalez, G. Tremiliosi-Filho, A. R. deAndrade, P. Olivi, K. B. Kokoh, *J. Power Sources* **167** (2007) 1
12. S. Delime, J.-M. Leger, C. Lamy, *J. Appl. Electrochem.* **29** (1999) 1249
13. A. O. Neto, M. J. Giz, J. Perez, E. A. Ticianelli, E. R. Gonzalez, *J. Electrochem. Soc.* **149** (2002) A272



14. J.-M. Leger, S. Rousseau, C. Coutanceau, F. Hahn, C. Lamy, *Electrochim. Acta* **50** (2005) 5118
15. W. J. Zhou, Z. H. Zhou, S. Q. Song, W. Z. Li, G. Q. Sun, P. Tsiakaras, Q. Xin, *Appl. Catal. B* **46** (2003) 273
16. A. K. Shukla, A. S. Arico, K. M. El-Khatib, H. Kim, P. L. Antonucci, V. Antonucci, *App. Surf. Sci.* **137** (1999) 20
17. A. S. Arico, V. Antonucci, N. Giordano, A. K. Shukla, M. K. Ravikumar, A. Roy, S. R. Barman, D. D. Sarma, *J. Power Sources* **50** (1994) 295
18. S. Mukerjee, J. McBreen, in *Proceedings of 2<sup>nd</sup> International Symposium on New Materials for Fuel Cells and Modern Battery Systems*, O. Savadoga, P. R. Roberge, Eds., Ecole Polytechnique, Montreal, 1997, p. 548
19. H. Li, G. Sun, L. Cao, L. Jiang, Q. Xin, *Electrochim. Acta* **52** (2007) 6622
20. W. J. Zhou, S. Q. Song, W. Z. Li, Z. H. Zhou, G. Q. Sun, Q. Xin, S. Douvartzides, P. Tsiakaras, *J. Power Sources* **140** (2005) 50
21. W. J. Zhou, S. Q. Song, W. Z. Li, G. Q. Sun, Q. Xin, S. Kontou, K. Poulianitis, P. Tsiakaras, *Solid State Ionics* **175** (2004) 797
22. J. H. Kim, S. M. Choi, S. H. Nam, M. H. Seo, S. H. Choi, W. B. Kim, *Appl. Catal. B* **82** (2008) 89
23. M. Zhu, G. Sun, Q. Xin, *Electrochim. Acta* **54** (2009) 1511
24. F. Colmati, E. Antolini, E. R. Gonzalez, *J. Power Sources* **154** (2006) 98
25. P. W. Albers, W. Weber, K. Kunzmann, M. Lopez, S. F. Parker, *Surf. Sci.* **602** (2008) 3611
26. S. Sen Gupta, S. Singh, J. Datta, *Mater. Chem. Phys.* **116** (2009) 223
27. R. F. B. De Souza, L. S. Parreira, D. C. Rascio, J. C. M. Silva, E. Teixeira-Neto, M. L. Calegario, E. V. Spinace, A. O. Neto, M. C. Santos, *J. Power Sources* **195** (2010) 1589
28. S. Mukerjee, J. McBreen, *J. Electrochem. Soc.* **146** (1999) 600
29. M. Arenz, V. Stamenković, B. B. Blizanac, K. J. Mayrhofer, N. M. Marković, P. N. Ross, *J. Catal.* **232** (2005) 402
30. T. Iwasita, *Electrochim. Acta* **47** (2002) 3663
31. I. Pašti, S. Mentus, *Mater. Chem. Phys.* **116** (2009) 94
32. P. Liu, A. Logadottir, J. K. Norskov, *Electrochim. Acta* **48** (2003) 3731
33. A. B. Anderson, E. Grantscharova, P. Schiller, *J. Electrochem. Soc.* **142** (1995) 1880
34. R. Alcalá, M. Mavrikakis, J. A. Dumesic, *J. Catal.* **218** (2003) 178
35. F. Vigier, C. Coutanceau, F. Hahn, E. M. Belgsir, C. Lamy, *J. Electroanal. Chem.* **563** (2004) 81
36. H. A. Gastaeiger, N. M. Marković, P. N. Ross, *Catal. Lett.* **36** (1996) 1
37. A. V. Tripković, K. Dj. Popović, J. D. Lović, V. M. Jovanović, S. I. Stevanović, D. V. Tripković, *Electrochem. Commun.* **11** (2009) 1030
38. Y. Yao, Q. Fu, Z. Zhang, H. Zhang, T. Ma, D. Tan, X. Bao, *Appl. Surf. Sci.* **254** (2008) 3808
39. S. Szabo, I. Bakos, F. Nagy, *J. Electroanal. Chem.* **271** (1989) 269
40. A. V. Tripković, G. Lj. Gojković, K. Dj. Popović, J. D. Lović, A. Kowal, *Electrochim. Acta* **53** (2007) 887
41. G. A. Camara, R. B. de Lima, T. Iwasita, *Electrochem. Commun.* **6** (2004) 812
42. A. Kowal, M. Li, M. Shao, K. Sasaki, M. B. Vukmirović, J. Zhang, N. S. Marinković, P. Liu, A. I. Frenkel, R. R. Adžić, *Nat. Mat.* **8** (2009) 325

43. A. Kowal, S. Lj. Gojković, K.-S. Lee, P. Olszewski, Y.-E. Sung, *Electrochem. Commun.* **11** (2009) 724
44. M. Li, A. Kowal, K. Sasaki, N. Marinković, D. Su, E. Korach, P. Liu, R. R. Adžić, *Electrochim. Acta* **55** (2010) 4331
45. J. D. Lović, A. V. Tripković, S. Lj. Gojković, K. Dj. Popović, D. V. Tripković, P. Olszewski, A. Kowal, *J. Electroanal. Chem.* **581** (2005) 294.